Proc. Natl. Acad. Sci. USA
Vol. 95, pp. 9773–9778, August 1998
Biochemistry

Determination of transmembrane topology of an inward-rectifying potassium channel from *Arabidopsis thaliana* based on functional expression in *Escherichia coli*

NOBUYUKI UOZUMI*†, TATSUNOSUKE NAKAMURA‡, JULIAN I. SCHROEDER§, AND SHOSHI MUTO*

*Bioscience Center, Nagoya University, Nagoya, 464-8601, Japan; ‡Faculty of Pharmaceutical Sciences, Chiba University, 1-33 Yayoi-cho, Inage-ku, Chiba 263-0022, Japan; and §Department of Biology and Center for Molecular Genetics, University of California at San Diego, La Jolla, CA 92093-0116

Communicated by André T. Jagendorf, Cornell University, Ithaca, NY, June 23, 1998 (received for review December 25, 1997)

ABSTRACT **We report here that the inward-rectifying potassium channels KAT1 and AKT2 were functionally expressed in K^+ uptake-deficient *Escherichia coli*. Immunological assays showed that KAT1 was translocated into the cell membrane of *E. coli*. Functional assays suggested that KAT1 was inserted topologically correctly into the cell membrane. In control experiments, the inactive point mutation in KAT1, T256R, did not complement for K^+ uptake in *E. coli*. The inward-rectifying K^+ channels of plants share a common hydrophobic domain comprising at least six membrane-spanning segments (S1–S6). The finding that a K^+ channel can be expressed in bacteria was further exploited to determine the KAT1 membrane topology by a gene fusion approach using the bacterial reporter enzymes, alkaline phosphatase, which is active only in the periplasm, and β-galactosidase. The enzyme activity from the alkaline phosphatase and β-galactosidase fusion plasmid showed that the widely predicted S1, S2, S5, and S6 segments were inserted into the membrane. Although the S3 segment in the alkaline phosphatase fusion protein could not function as an export signal, the replacement of a negatively charged residue inside S3 with a neutral amino acid resulted in an increase in alkaline phosphatase activity, which indicates that the alkaline phosphatase was translocated into the periplasm. For membrane translocation of S3, the neutralization of a negatively charged residue in S3 may be required presumably because of pairing with a positively charged residue of S4. These results revealed that KAT1 has the common six transmembrane-spanning membrane topology that has been predicted for the Shaker superfamily of voltage-dependent K^+ channels. Furthermore, the functional complementation of a bacterial K^+ uptake mutant in this study is shown to be an alternative expression system for plant K^+ channel proteins and a potent tool for their topological analysis.**

Potassium is a major essential nutrient in higher plants and plays important physiological roles for turgor maintenance, enzyme activity, stomatal movements, growth, and development (1, 2). Multiple pathways for K^+ uptake exist in plants to satisfy various cellular requirements for K^+ under many different types of soil and environmental conditions (3–5). *Arabidopsis* inward-rectifying potassium channel genes, *KAT1* (6) and *AKT1* (7), were isolated from *Arabidopsis* cDNA libraries by functional complementation of a K^+ uptake-deficient yeast mutant. Further cloning studies on plant inward-rectifying K^+ (K^+_{in}) channels have revealed two new cDNAs coding for K^+_{in} channels, *AKT2/AKT3* (8, 9) and *KST1* (10). Plant K^+_{in} channels have been analyzed by heterologous expression systems using yeast and/or *Xenopus* oocytes. Plant K^+_{in} channels were characterized as hyperpolarization-activated (inward-rectifying) K^+ channels that display voltage- and time-dependent activation, and K^+ selectivity properties (9, 11–13). These channels have six putative membrane-spanning segments, a typical voltage sensor segment (S4), and a K^+-selective pore (H5 or P) domain (8–10, 14–19). Interestingly, plant K^+_{in} channels are structurally similar to depolarization-activated K^+ (K^+_D) channels in animals, despite the opposite voltage-dependent activation of the two channel classes (20). Functional chimeric channels of a plant K^+_{in} channel, KAT1 and an animal K^+_D channel, Xsha2, therefore, could be formed (14). However, little direct evidence has been reported on the membrane topology of plant K^+_{in} channels and animal K^+_D channels. Recently, the structure of a K^+ channel that has two transmembrane segments was determined from x-ray diffraction data with a resolution of 3.2 Å (21). To our knowledge, the complete membrane topology of a voltage-gated K^+ channel has not yet been experimentally determined.

Several approaches have been reported for the determination of the topology of eukaryotic membrane proteins in addition to x-ray diffraction analysis. Glycosylation site tagging has been applied to study the topology of the kainate receptor (22), nicotinic acetylcholine receptors (23), H^+, K^+-ATPase (24), and glutamate receptors (25). On the other hand, Wang *et al.* (26) used antibodies directed against a synthetic peptide of the β-adrenergic receptor to define its topology.

A gene fusion approach with alkaline phosphatase (PhoA) has been reported to study prokaryote membrane transporters (27–34). PhoA is enzymatically active when it is exported across the inner membrane into the periplasm (35), whereas PhoA remains inactive in the cytoplasm because disulfide bond formation, essential for enzymic activity, does not occur (36). The PhoA activity therefore indicates the orientation of PhoA with respect to the membrane. The PhoA fusion approach in *Escherichia coli* has been applied to examine the topology of the β-adrenergic receptor (37) and cyclic nucleotide-gated ion channels (38).

Because bacteria have no subcellular membranes, the membrane proteins that are normally expressed in the plasma membrane or endomembranes of eukaryotic cells may be inserted into the plasma membrane of bacterial cells. If membrane proteins can be expressed in the bacterial membrane, the PhoA fusion method would be feasible for topological analyses in *E. coli*. However, there are limited reports on functional expression of eukaryote membrane proteins in *E. coli*. Bibi *et al.* (39) succeeded in functionally expressing a mouse multidrug-resistance protein in *E. coli*. The plant K^+ transporter homologous to the *E. coli kup* gene complemented

The publication costs of this article were defrayed in part by page charge payment. This article must therefore be hereby marked "*advertisement*" in accordance with 18 U.S.C. §1734 solely to indicate this fact.

Abbreviations: K^+_{in}, inward-rectifying K^+; K^+_D, outward-rectifying K^+; PhoA, alkaline phosphatase; LacZ, β-galactosidase.

†To whom reprint requests should be addressed. e-mail: uozumi@agr.nagoya-u.ac.jp.

K^+ uptake deficiencies involving Kup system mutations in *E. coli* (40).

In the present study, we report that the *KAT1* and *AKT2* cDNAs complemented a K^+ uptake-deficient triple *E. coli* mutant (41). This complementation and control experiments suggested that KAT1 was synthesized and then placed in the proper conformation in *E. coli* cell membranes. On the basis of this complementation, we have pursued the expression of a set of KAT1-PhoA and KAT1-β-galactosidase (LacZ) fusions to determine their topology in the bacterial membrane and the requirements for correct insertion into the membrane.

MATERIALS AND METHODS

Expression of KAT1 and AKT2 in *E. coli*. The *Kpn*I–*Pst*I fragments of *KAT1* cDNA from the plasmid constructed previously (14, 15) and the *Bam*HI–*Kpn*I fragment produced by PCR products were ligated into the *Bam*HI–*Pst*I sites of pPAB404 that was kindly provided by W. Epstein (University of Chicago) (29). The resultant plasmid containing the entire *KAT1* coding region was designated pPAB-KAT1. pPAB-D141V-KAT1, in which aspartate at position 141 was replaced with valine in pPAB-KAT1, was constructed by a site-directed mutagenesis procedure based on PCR (42). pPAB-T256R-KAT1, in which threonine at position 256 was replaced with arginine in pPAB-KAT1, was generated from the plasmid with T256R as reported previously (15). The DNA between the *Hin*dIII site located upstream of the initiation codon of the *AKT2* cDNA and the *Xho*I site downstream of the stop codon in pBlueScript KSII was constructed previously (8). This plasmid was named pBS-AKT2 in this study. The plasmids were expressed in *E. coli* LB2003, which lacks the three K^+ uptake systems, Trk (TrkG and TrkH), Kup (TrkD), and Kdp (a kind gift from E. P. Bakker, Universität Osnabrück, Germany) (41, 43). The *E. coli* strain was grown at 30°C on liquid medium with 0.5 mM isopropyl β-D-thiogalactopyranoside as described elsewhere (29, 44). K^+ concentrations were determined by flame photometry using a Perkin–Elmer 403 atomic absorption spectrophotometer (44, 45).

Construction of KAT1 Fusion Protein. To construct the KAT1-PhoA fusion protein, pPAB404, which contains the *Bam*HI–*Pst*I cloning sites for PhoA fusion, was employed as the fusion vector according to Buurman *et al.* (29) and Enomoto *et al.* (33). The pPAB-KAT1 served as the template for PCR amplification to obtain the *Bam*HI–*Pst*I DNA fragments encoding partial KAT1 polypeptides from the N terminus to the fusion joints. The sense primer annealed to the sequence 12 bp upstream of the start of the KAT1 coding sequence and contained the *Bam*HI-specific sequence. The antisense primers served as distal in-frame *Pst*I site primers for selected fusion joints. The PCR-amplified DNA fragments were digested with *Bam*HI and *Pst*I, and then cloned into the *Bam*HI–*Pst*I sites of pPAB404. The resultant plasmids were designated pXxxx-PhoA, where X is the one-letter symbol of the amino acid residue at the fusion joint and xxx is the residue position number. For R322-PhoA constructs, the *Xba*I site at the amino acid position 322 in pPAB-KAT1 was ligated to the *Xba*I site of pPAB404. The pD141V-E161-PhoA (replacement of aspartate with valine at position 141 in pE161-PhoA) and pH373V-R383V-E396-PhoA (replacement of histidine at position 373 and arginine at position 383 with valines in pE396-PhoA) were constructed by a site-directed mutagenesis procedure based on PCR (42). All PCR-generated DNA fragments were verified by DNA sequencing. The KAT1-LacZ fusion protein was constructed by exchange of the phoA gene with the lacZ gene as described by Buurman *et al.* (29). The PhoA fusions cloned in pPAB404 were digested with *Bam*HI and *Dra*I and cloned into *Bam*HI–*Sma*I sites in pJLZ104, which was a kind gift from W. Epstein (University of Chicago). The resultant plasmids, pXxxx-LacZ, were designed to encode LacZ fused with KAT1 in frame. KAT1-PhoA and KAT1-LacZ fusion proteins encoded in pXxxx-PhoA plasmids and pXxxx-LacZ plasmids are indicated as Xxxx-PhoA and Xxxx-LacZ proteins, respectively.

Expression of Fusion Constructs and Enzyme Assay. The PhoA and LacZ fusions were expressed in *E. coli* UT5600 (33, 39) and in MC4100 (46). The cells were grown in Luria–Bertani medium containing 50 μg/ml ampicillin, 0.5 mM isopropyl β-D-thiogalactopyranoside, and 1.5% agar for 16 h at 30°C. The chromogenic indicators 5-bromo-4-chloro-3-indolyl phosphate (toluidine salt, XP) at 40 μg/ml and 1 mM 5-bromo-4-chloro-3-indolyl β-D-galactoside (X-Gal) were used for PhoA and LacZ, respectively. Cells were grown on solid medium overnight, harvested, washed in 50 mM phosphate buffer (pH 7.0), and resuspended in the same buffer. The suspension containing 0.1 mg of fresh cells per ml was frozen and thawed and disrupted by sonication or French press. Cell debris was removed by centrifugation for 5 min at $16{,}000 \times g$. Membranes were collected by ultracentrifugation for 30 min at $100{,}000 \times g$ and resuspended in 50 mM phosphate buffer (pH 7.0) at 0.1 mg of fresh cells per ml. The membrane fraction was used for measurement of LacZ activities. LacZ activities were measured as described (47). PhoA activities were determined according to Brickman and Beckwith (48). The crude proteins in the membrane fraction were separated by electrophoresis on SDS/8 or 10% polyacrylamide gels and transferred electrophoretically to polyvinylidene difluoride membranes (49). Immunoblot detection was performed with anti-*E. coli* PhoA antibody (Rockland, Gilbertsville, PA) and PhoA-conjugated anti-rabbit IgG (Dako) for detection of PhoA fusion proteins and anti-*E. coli* LacZ antibody (Chemicon) and a horseradish peroxidase-conjugated protein G (Zymed) for detection of LacZ fusion proteins. Protein concentration was measured by the method of Lowry *et al.* (50) or of Bradford (51).

RESULTS

Functional Complementation of the *E. coli* Mutant by KAT1 and AKT2. *E. coli* LB2003, lacking the K^+ uptake systems, Trk, Kup, and Kdp, could not grow on K^+-limiting medium (Fig. 1) (41). This triple K^+ transport deficient system requires 25 mM K^+ for half-maximal cell growth (43). As shown in Fig. 1, the growth of cells with empty vectors, pPAB404 and pBluescript KSII, in medium with 10.4 mM K^+ at the initial concentration reached <0.2 OD at 600 min. In contrast, cells expressing the higher plant K^+ channels genes, pPAB-KAT1 and pBS-AKT2, grew up to the full-growth level within 540 min in medium containing 8.4 mM K^+. The length and nature of the amino acid side chain at position 256 in KAT1 is important for cation selectivity and a mutant, T256R, did not confer significant K^+ uptake and growth of the K^+ uptake deficient yeast (15). For *E. coli* complementation tests, the T256R mutant (pPAB-T256R-KAT1) exhibited a similar growth rate to cells with empty vectors (Fig. 1). These results showed functional complementation of an *E. coli* mutant with KAT1 and AKT2.

To confirm translocation of KAT1 into the cell membrane of *E. coli*, KAT1 tagged with PhoA and with LacZ was detected by Western blot analysis. Tagged KAT1 could be detected in the membrane fraction (details of the experiments are described later). These results suggested that KAT1 was both translocated into the cell membrane and expressed with inward transporting K^+ activity.

Hydropathy of KAT1. The functional expression of plant K^+ channels in the *E. coli* membrane indicates that it is possible to determine the KAT1 topology in the *E. coli* system. Using the Hopp and Woods criterion (52), several hydrophobic regions in KAT1 are shown in Fig. 2 (6). The H5 segment between S5 and S6 is a hydrophobic region, which forms the pore of K^+_{in} channels based on several results obtained from site-directed mutagenesis in this region and structural analysis

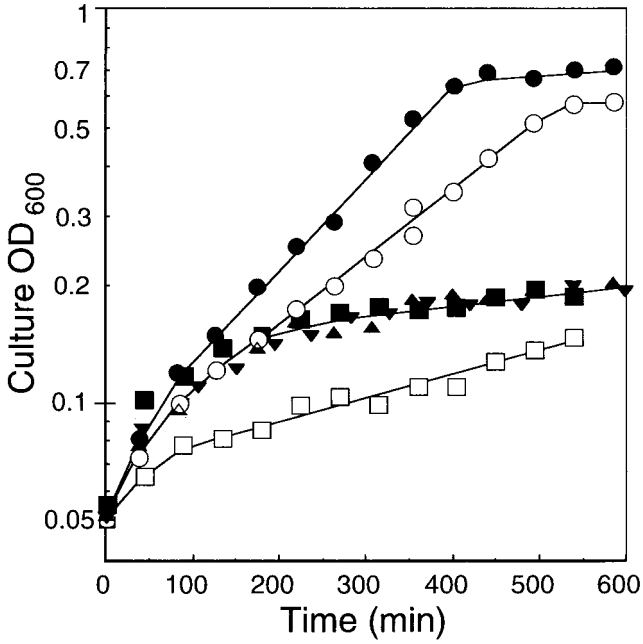

FIG. 1. Effect of K^+ concentrations on the growth of the K^+ uptake-deficient *E. coli* mutant strain LB2003 with pPAB-KAT1 (●), pBS-AKT2 (○), pPAB-D141V-KAT1 (▲), pPAB-T256R-KAT1 (▼), and vector plasmids, pPAB404 (■) and pBluescript KSII (□) in liquid culture. The initial K^+ concentrations were measured by flame photometry. ●, 8.5 mM; ○, 8.5 mM; 8.8 mM; ▲, 7.6 mM; ▼, 10.4 mM; □, 10.4 mM

(see Discussion). This region also contains the GYG consensus amino acid sequence for pore formation in animal K_D^+channels (20). In the C-terminal region between S6 and the C terminus, there are both a highly hydrophobic segment, named S7 in this report (residues 363–390), and a putative cyclic nucleotide-binding domain (residues 386–449) (6) as shown in Fig. 2. S7 is a typical hydrophobic sequence that does not exist in animal K_D^+ channels. The S4 region, which shows low hydrophobicity in the hydropathy plot (Fig. 2), has several positively charged amino acids that are considered to be components of the voltage sensor. Two negatively charged residues (D95 and D105) in S2 and one negatively charged residue (D141) in S3 exist in KAT1 (6). The space between D95 and D105 is also conserved between plant K_{in}^+ channels and animal K_D^+ channels (6, 53). According to predictions by the TopPredII algorithm (53), S1, S2, S3, S5, H5, S6, and S7, but not S4, form transmembrane segments.

PhoA and LacZ Activities from KAT1 Fusion Plasmids. To assess which of the segments (S1–S7 and H5) actually traverse the membrane, and to assemble the transmembrane topology of KAT1, pXxxx-PhoA plasmids encoding eight different PhoA fusion proteins were constructed and transformed into UT5600, a commonly employed host for PhoA assays (33, 39). The fusion sites were selected as amino acids in or adjacent to the presumed loops located between the predicted transmembrane segments as shown in Fig. 2. PhoA is active only when it is translocated to the periplasm (extracellular membrane side) (35, 36). Fusions D95-PhoA, G232-PhoA, and E273-PhoA produced high PhoA activities, indicating a periplasmic location for the PhoA, whereas K128-PhoA, E161-PhoA, K200-PhoA, R322-PhoA, and E396-PhoA showed very low activities, indicating a cytoplasmic location for PhoA (Table 1). All KAT1-fusion products conferring higher PhoA activities were detected in the membrane fraction by Western blot analysis (Fig. 3*A*). On the other hand, *E. coli* with the lower PhoA activities did not show PhoA bands in the membrane fraction (Fig. 3*A*) or in the soluble fraction (data not shown).

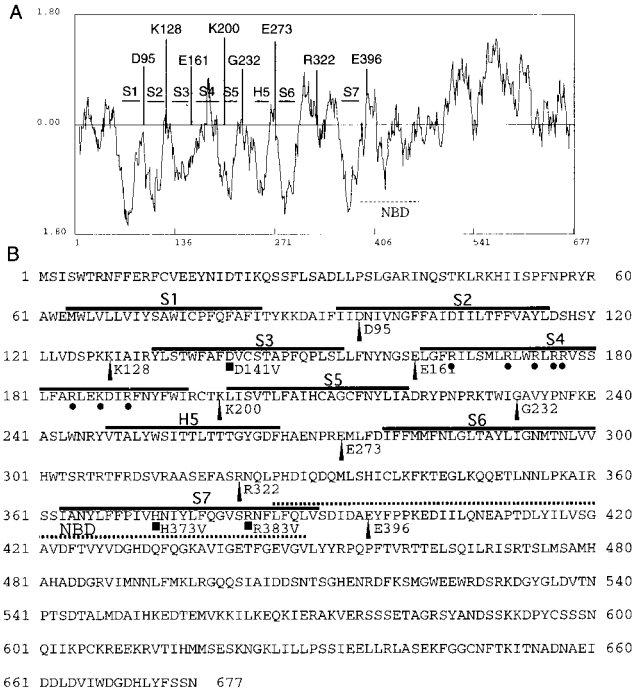

FIG. 2. Hydropathy plot and deduced transmembrane domains of KAT1 (*A*) and deduced amino acid sequence (*B*). Hydrophobicity plot was generated by the method of Hopp and Woods with a window of 13 amino acids (6, 52). Negative values show hydrophobic regions. The positions of fusion sites selected for PhoA fusion are indicated by the bars (*A*) and arrowheads (*B*). ■ Shows the amino acids that were replaced with valines (*Materials and Methods*). ● Represents the positively charged amino acids in the putative S4 segment. The putative transmembrane segments (S1, S2, S3, S4, S5, H5, S6, and S7) are indicated by horizontal bars. The horizontal dotted line represents the putative nucleotide-binding domain (NBD).

The undetectable level of the fusions could be due to either degradation of these protein products in the cytoplasm or a lack of gene expression. Examples of unstable PhoA proteins that were fused with bacterial membrane proteins, including a mechanosensitive channel (32), the Kdp transport ATPase (29), and ATP-binding cassette transporter (54), have been reported. To demonstrate the instability of PhoA in the cytoplasm and to exclude the possibility of low gene expression, fusions to LacZ were constructed by replacement of PhoA with LacZ (Fig. 3*B* and Table 1). LacZ activity was expressed at higher, though different, levels in all constructs when compared with the controls (Table 1). All fusion proteins were associated with the membrane fraction as shown by Western blot analysis (Fig. 3*B*). These results suggested that PhoA domain was unstable or proteolytically removed from membrane domain when it was located in the cytoplasm (29,

Table 1. Enzyme activities of PhoA and LacZ fusion proteins

Fusion	PhoA activity, units	LacZ activity, units
None	0.63 ± 0.026	0.0067 ± 0.015
D95	33 ± 8.3	1.5 ± 0.11
K128	0.93 ± 0.069	3.6 ± 0.37
E161	0.90 ± 0.011	5.4 ± 0.32
D141V-E161	36 ± 3.0	1.8 ± 0.20
K200	0.52 ± 0.045	1.4 ± 0.070
G232	21 ± 2.7	1.6 ± 0.051
E273	21 ± 2.3	1.7 ± 0.046
R322	0.79 ± 0.13	0.45 ± 0.028
E396	0.58 ± 0.027	3.3 ± 0.14
H373V-R383V-E396	2.2 ± 0.020	3.3 ± 0.96

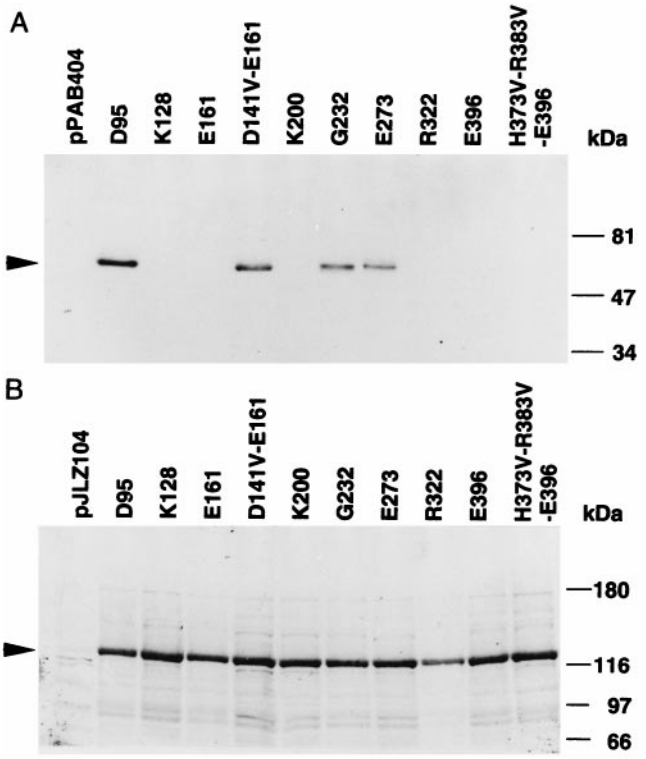

FIG. 3. Immunoblot analysis for KAT1-PhoA fusion proteins expressed in *E. coli* UT5600 (*A*) and KAT1-LacZ fusion proteins expressed in *E. coli* MC4100 (*B*). Transformed *E. coli* were grown on solid medium for 1 day, and membranes were prepared as described in the text. Membrane proteins (10 μg) were subjected to SDS/10% (*A*) or SDS/8% (*B*) polyacrylamide gel electrophoresis followed by Western blotting.

32, 54). Based on the above data, we concluded that the S1, S2, S5, and S6 segments traverse the membrane.

Export Efficiency of the KAT1 Fusion with Mutation in S3. The KAT1 S3 segment possesses one acidic residue, an aspartate at position 141. This residue may impair the translocation of the S3 segment in E161-PhoA because of the absence of the S4 segment in this construct. Henn *et al.* (38) reported that the charged amino acid located in the S3 transmembrane segments of cyclic nucleotide-gated ion channels interfered with traversal of this membrane segment. They elegantly overcame this limitation by replacing the charged amino acid with a neutral amino acid. Accordingly, we constructed a fusion PhoA plasmid that has a site-directed mutation, D141V. *E. coli* expressing the resultant fusion, D141V-E161-PhoA, exhibited a marked increase in PhoA activity compared with E161-PhoA (Table 1). The D141V-E161-PhoA was detected by Western blot analysis although E161-PhoA was not detected (Fig. 3*A*). In addition, in the LacZ fusion experiment, the LacZ activity of D141V-E161-LacZ was decreased by 3-fold compared with that of E161-LacZ (Table 1 and Fig. 3*B*). The reduction in the LacZ activity may have occurred because the LacZ domain immediately following the S3 in D141V-E161-LacZ might be embedded in the membrane, which could reduce enzyme activity (35). These results correlate with those of the PhoA fusion. These data indicate that replacement of the charged residue by a neutral residue at position 141 allows PhoA translocation to the periplasm. The neutralization of the D141 charge is required for S3 to have a functional export signal. To confirm the contribution of D141 to expression of functional K^+ uptake activity, growth tests of *E. coli* LB2003 containing pPAB-D141V-KAT1 were performed (Fig. 1). The replacement D141V removed the K^+ uptake complementation. This suggested that interaction of D141 with the other residues in

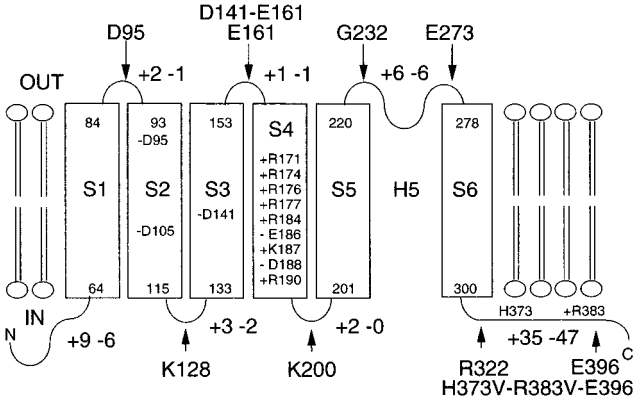

FIG. 4. Proposed membrane topology of KAT1 as derived from PhoA and LacZ fusions. Transmembrane segments (S1–S6) are shown as open rectangles. The position of charged amino acids in loops are indicated by + (Arg and Lys) and − (Asp and Glu). The *phoA* and *lacZ* gene fusion positions are indicated by arrows.

S4 might be needed for proper function of KAT1 in *E. coli*, in analogy to the interaction of charged residues of S3 and S4 in animal K_D^+ channels (55, 56).

Localization of S7. As described above, S7 did not function as an export signal, but two positively charged amino acids reside in S7, histidine at position 373 and arginine at position 383 (Fig. 2*B*). Therefore, these two sites were replaced with valines simultaneously in E396-PhoA to estimate whether negative residues affect membrane insertion as shown above for S3. The PhoA activity of H373V-R383V-E396-PhoA increased ≈3.8× compared with that of E396-PhoA (Table 1). However, the activity was substantially lower than all fusions predicted to face the periplasm (Table 1). In addition, the LacZ activity of H373V-R383V-E396-LacZ was the same as that of E396-LacZ. These data suggests that S7 is not a transmembrane segment. Fig. 4 shows the topological model generated for KAT1 derived from these data. KAT1 expressed in *E. coli* spans the membrane six times.

DISCUSSION

As a result of the functional expression of KAT1 in the *E. coli* membrane and lack of function of the inactive T256R mutant (15), we were prompted to determine the KAT1 topology by PhoA-fusion analysis, because the complete membrane topology of voltage-gated K^+ channels had not yet been experimentally determined. Note that locations of individual segments of animal K_D^+ channels have been determined (20). The strong hyperpolarization-induced activation of KAT1 precludes steady-state outward K^+ currents as shown in *Xenopus* oocytes (12, 57). If KAT1 were inserted into the *E. coli* membrane in the opposite orientation, the K^+ channel would be expected not to complement the K^+ uptake deficiency. The functional expression of KAT1 suggests that KAT1 is expressed in the proper conformation in the membrane. Several studies have reported expression of eukaryotic membrane proteins in the bacterial cell membrane (37–40, 54). To our knowledge, there are a few reports that demonstrate functional expression of a eukaryotic protein in *E. coli* (39, 40). Because modifications such as glycosylation are lacking in *E. coli*, certain eukaryotic membrane proteins may fail to take their active form in bacteria. In the case of the multidrug resistance protein (P-glycoprotein) (39), the protein functioned in its unglycosylated form in *E. coli*. Although KAT1 and AKT2 complemented the *E. coli* mutant, LB2003, the electrical properties expressed in the *E. coli* membrane remain unknown.

Assessment of enzyme activities in *E. coli* with a series of PhoA- and LacZ-fusion plasmids enabled us to identify S1, S2,

S5, and S6 as transmembrane segments. The predicted pore-forming sequence, H5, between G232 in the S5–H5 loop and E273 in the H5-S6 loop shows relatively high hydrophobicity from the hydropathy profile in Fig. 2. The data in Table 1 and Fig. 3 showed that G232 and E273 face the extracellular space. The pore-forming ability of KAT1 has been supported by data showing that site-directed mutations in the H5 domain of KAT1 affect cation selectivity and cation block (15, 16, 18, 19).

Sequence comparisons between plant K^+_{in} channels and animal K^+_D channels has revealed that the two types of channels share typical similarities in the hydrophobic core regions, S2 and S3, as well as in the voltage sensor S4 (6–9). The two negatively charged residues in S2 (D95 and D105) and the negatively charged aspartic acid in S3 (D141), which are all highly conserved among animal K^+_D channels (20), are also conserved in plant K^+_{in} channels (Fig. 2). These negatively charged amino acids interact with some of the positively charged amino acids in S4 to contribute to the function of the voltage sensor in animal K^+_D channels (55, 56, 58). The neutralization of electrostatic interactions leads to packing of S2, S3, and S4 segments and mediates the proper folding of the protein (56). The failure of *E. coli* complementation by pPAB-D141V-KAT1 may be attributable to a disordered KAT1 structure. The replacement of D141 by valine in E161-PhoA artificially created a new transmembrane segment. The pD141V-E161-PhoA construct suggests that the neutralization of the charged amino acid is necessary for membrane traversal by S3 in KAT1 (Table 1). Our results are similar to the reports by Henn *et al.* (38). Neutralization of the corresponding charged amino acid in the S3 segment of the PhoA-fused cyclic nucleotide-gated ion channels allowed S3 to traverse the membrane. It was proposed that in native channels, the negatively charged residues of S3 are compensated for by the positively charged residues in S4, allowing S3 and S4 to be simultaneously inserted into the membrane. By cysteine substitution methods in combination with specific cysteine affinity labeling, Mannuzzu *et al.* (59) showed that the S3–S4 loop faces the extracellular space in animal K^+_D channels. Our data also appear to be consistent with models in which charged residues of S3–S4 of KAT1 interact.

One additional candidate for a putative transmembrane segment, S7, was analyzed (Fig. 2). However, the R322-PhoA and E396-PhoA constructs did not confer detectable positive PhoA activity in *E. coli*, whereas R322-LacZ and E396-LacZ proteins were translocated into the membrane fraction (Table 1). Furthermore, neutralization of two charged residues in S7 did not enhance significant export efficacy. Therefore, S7 was predicted to face the cytoplasm. This region is located in the vicinity of the putative cyclic nucleotide-binding domain, which is also predicted to be in the cytoplasm (6).

Our results provide evidence for a model with six membrane-spanning domains, and two cytoplasmic loops, as shown in Fig. 4. The loops of S2–S3 and S4–S5 have a net positive charge. This is consistent with the "positive inside" rule for protein orientation (60).

The present data experimentally establish the membrane topology of a voltage-dependent K^+ channel. Furthermore, we show here that the membrane topology of the hyperpolarization-activated KAT1 K^+ channel is the same as that predicted for depolarization-activated K^+ channels in animal cells (20). This report shows that higher plant membrane proteins can be analyzed and functionally expressed in the *E. coli* expression system.

We thank André T. Jagendorf (Cornell University, Nagoya University), Michael Conlon (Nagoya University), and Angelica Alvarez-Nakase (Nagoya University) for helpful suggestions and reading of the manuscript. We greatly appreciate the kind gifts of plasmids pPAB404 and pJLZ104 from Wolfgang Epstein (University of Chicago). We are also grateful to Evert P. Bakker (Universität Osnabrück) for the generous gift of *E. coli* LB2003, and Akiko Nishimura (National Institute of Genetics, Mishima, Japan) for the gift of *E. coli* MC4100. This work was supported in part by a grant-in-aid for scientific research from the Ministry of Education, Science, Sports and Culture of Japan, and the Salt Science Research Foundation and in part by Department of Energy Grant DE-FGO3-94-ER20148.

1. Schroeder, J. I., Ward, J. M. & Gassmann, W. (1994) *Annu. Rev. Biophys. Biomol. Struct.* **23,** 441–471.
2. Maathius, F. J. M. & Sanders, D. (1996) *Physiol. Plant.* **96,** 158–168.
3. Epstein, W., Rains, D. W. & Elzam, O. E. (1963) *Proc. Natl. Acad. Sci. USA* **49,** 684–692.
4. Kochian, L. V. & Lucas, W. J. (1988) *Adv. Not. Res.* **15,** 93–178.
5. Newman, I. A., Kochian, L. V., Grusak, M. A. & Lucas, W. J. (1987) *Plant Physiol.* **84,** 1177–1184.
6. Anderson, J. A., Huprikar, S. S., Kochian, L. V., Lucas, W. J. & Gaber. R. F. (1992) *Proc. Natl. Acad. Sci. USA* **89,** 3736–3740.
7. Sentenac, H., Bonneaud, N., Minet, M., Lacroute, F., Salmon, J. M., Gaymard, F. & Grignon, C. (1992) *Science* **256,** 663–665.
8. Cao, Y., Ward, J. M., Kelly, W. B., Ichida, A. M., Gaber, R. F., Anderson, J. A., Uozumi, N., Schroeder, J. I. & Crawford. N. M. (1995) *Plant Physiol.* **109,** 1093–1106.
9. Ketchum, K. A. & Slayman, C. W. (1996) *FEBS Lett.* **378,** 19–26.
10. Müller-Röber, B., Ellenberg, J., Provart, N., Willmitzer, L., Busch, H., Becker, D., Dietrich, P., Hoth, S. & Hedrich, R. (1995) *EMBO J.* **14,** 2409–2416.
11. Schroeder, J. I., Raschke, K. & Neher, E. (1987) *Proc. Natl. Acad. Sci. USA* **84,** 4108–4112.
12. Schachtman, D. P., Schroeder, J. I., Lucas, W. J., Anderson, J. A. & Gaber, R. F. (1992) *Science* **258,** 1654–1658.
13. Hoshi, T. (1995) *J. Gen. Physiol.* **105,** 309–328.
14. Cao, Y., Crawford. N. M. & Schroeder, J. I. (1995) *J. Biol. Chem.* **270,** 17697–17701.
15. Uozumi, N., Gassmann, W., Cao, Y. & Schroeder, J. I. (1995) *J. Biol. Chem.* **270,** 24276–24281.
16. Becker, D., Dreyer, I., Hoth, S., Reid, J. D., Busch, H., Lehnen, M., Palme, K. & Hedrich, R. (1996) *Proc. Natl. Acad. Sci. USA* **93,** 8123–8128.
17. Marten, I. & Hoshi, T. (1997) *Proc. Natl. Acad. Sci. USA* **94,** 3448–3453.
18. Nakamura, R. L., Anderson, J. A. & Gaber, R. F. (1997) *J. Biol. Chem.* **272,** 1011–1018.
19. Ichida, A. M. & Schroeder, J. I. (1996) *J. Membr. Biol.* **151,** 53–62.
20. Jan, L. Y. & Jan, Y. N. (1992) *Cell* **69,** 715–718.
21. Doyle, D. A., Cabral, J. M., Pfuetzner, R. A., Kuo, A., Gulbis, J. M., Cohen, S. L., Chait, B. T. & MacKinnon, R. (1998) *Science* **280,** 69–77.
22. Wo, Z. G. & Oswald, R. E. (1994) *Proc. Natl. Acad. Sci. USA* **91,** 7154–7158.
23. Chavez, R. A. & Hall, Z. W. (1991) *J. Biol. Chem.* **266,** 15532–15538.
24. Bamberg, K. & Sachs, G. (1994) *J. Biol. Chem.* **269,** 16909–16919.
25. Hollmann, M., Maron, C. & Heinemann, S. (1994) *Neuron* **13,** 1331–1341.
26. Wang, H., Lipfert, L., Malbon, C. C. & Bahouth, S. (1989) *J. Biol. Chem.* **264,** 14424–14431.
27. Wu, J., Tisa, L. S. & Rosen, B. P. (1992) *J. Biol. Chem.* **267,** 12570–12576.
28. Zimmann, P., Puppe, W. & Altendorf, K. (1995) *J. Biol. Chem.* **270,** 28282–28288.
29. Buurman, E. T. Kim, K.-T. & Epstein, W. (1995) *J. Biol. Chem.* **270,** 6678–6685.
30. Danielsen, S., Boyd, D. & Neuhard, J. (1995) *Microbiology* **141,** 2905–2913.
31. Johansson, M. & von Heijne, G. (1996) *J. Biol. Chem.* **271,** 25912–25915.
32. Blount, P., Sukharev, S. I., Moe, P. C., Schroeder, M. J., Guy, H. R. & Kung, C. (1996) *EMBO J.* **15,** 4798–4805.
33. Enomoto, H., Unemoto, T., Nishibuchi, M., Padan, E. & Nakamura, T. (1998) *Biochim. Biophys. Acta* **1379,** 77–86.
34. Froshauer, S., Green, G. N., Boyd, D., McGovern, K. & Beckwith, J. (1988) *J. Mol. Biol.* **200,** 501–511.
35. Manoil, C. & Beckwith, J. (1986) *Science* **233,** 1403–1408.
36. Derman, A. I. & Beckwith, J. (1991) *J. Bacteriol.* **173,** 7719–7722.
37. Lacatena, R. M., Cellini, A., Scavizzi, F. & Tocchini-Valentini, G. P. (1994) *Proc. Natl. Acad. Sci. USA* **91,** 10521–10525.

38. Henn, D. K., Baumann, A. & Kaupp, U. B. (1995) *Proc. Natl. Acad. Sci. USA* **92,** 7425–7429.
39. Bibi, E., Cros, P. & Kaback H. R. (1993) *Proc. Natl. Acad. Sci. USA* **90,** 9209–9213.
40. Kim, E. J., Kwak, J. M. Uozumi, N. & Schroeder, J. I. (1998) *Plant Cell* **10,** 51–62.
41. Stumpe, S., Schlösser, A., Schleyer, M. & Bakker, E. P. (1996) *in Handbook of Biological Physics,* eds. Konings, W. N., Kaback, H. R. & Lolkema, J. S. (Elsevier, Amsterdam), Vol. **2,** pp. 473–499.
42. Higuchi, R. (1990) *in PCR Protocols: A Guide to Methods and Applications,* eds. Innis, M. S., Gelfand, D. H., Sninsky, J. J. & White, T. J. (Academic, Orlando, FL), pp. 177–183.
43. Epstein, W. & Kim, A. S. (1971) *J. Bacteriol.* **108,** 639–644.
44. Nakamura, T., Yamamuro, N., Stumpe, S., Unemoto, T. & Bakker, E. P. (1998) *Microbiology*, in press.
45. Bakker, E. P. & Mangerich, W. E. (1981) *J. Bacteriol.* **147,** 820–826.
46. Schweizer, H. & Boos, W. (1983) *Mol. Gen. Genet.* **192,** 293–294.
47. Sambrook, J., Fritsch, E. F. & Maniatis, T. (1989) *Molecular Cloning: A Laboratory Manual* (Cold Spring Harbor Lab. Press, Plainview, NY), 2nd Ed.
48. Brickman, E. & Beckwith, J. (1975) *J. Mol. Biol.* **96,** 307–316.
49. Simogawara, K. & Muto, S. (1992) *Plant Cell Physiol.* **30,** 9–16.
50. Lowry, O. H., Rosebrough, N. J., Farr, A. L. & Randall, R. L. (1951) *J. Biol. Chem.* **193,** 265–275.
51. Bradford, M. M. (1976) *Anal. Biochem.* **72,** 248–254.
52. Hopp, T. P. & Woods, K. R. (1981) *Proc. Natl. Acad. Sci. USA* **78,** 3824–3828.
53. von Heijne, G. (1992) *J. Mol. Biol.* **225,** 487–494.
54. Gileadi, U. & Higgins, C. F. (1997) *J. Biol. Chem.* **272,** 11103–11108.
55. Papazian, D. M., Shao, X. M., Seoh, S.-A., Mock, A. F., Huang, Y. & Wainstock, D. H. (1995) *Neuron* **14,** 1293–1301.
56. Tiwari-Woodruff, S. K., Schulteis, C. T., Mock, A. F. & Papazian, D. M. (1997) *Biophys. J.* **72,** 1489–1500.
57. Sussman, M. R. (1994) *Annu. Rev. Plant Physiol.* **45,** 211−234.
58. Seoh, S.-A., Sigg, D., Papazian, D. M. & Bezanilla, F. (1996) *Neuron* **16,** 1159–1167.
59. Mannuzzu, L. M., Moronne, M. M. & Isacoff, E. Y. (1996) *Science* **271,** 213–216.
60. von Heijne, G. (1986) *EMBO J.* **5,** 3021–3027.